Rheology and Applications of Particulate Composites in Additive Manufacturing

Bin Xia, Paul S. Krueger *

Department of Mechanical Engineering, Bobby B. Lyle School of Engineering, Southern Methodist University, Dallas, TX 75275

Abstract

To provide different functionalities such as electrical conductivity or magnetic permeability, particulate composites have been utilized widely in additive manufacturing. These types of materials are usually formulated with different functional particles and shear thinning non-Newtonian fluids such as polymer melts and silicone. The materials are viscous non-Newtonian suspensions during formulation and printing, and their rheology is a key factor for the processing. This paper will concentrate on suspensions with micron-sized particles, and discuss the rheology and overall flow behavior in capillaries scaled appropriately for additive manufacturing applications (around 1 mm ID). Micron size glass beads and shear thinning silicone are used to demonstrate the impact of particle volume fraction on the shear thinning behavior. The impact of particle and capillary size on viscosity and jamming conditions will be discussed. Previous models based on Newtonian fluids and in free flowing conditions will also be reviewed and compared.

Key words: particulate composite, viscosity, rheology, particulate suspension, additive manufacturing, 3-D printing, capillary flow, jamming condition, volume fraction, particle size

1. Introduction

Particulate composites consist of a matrix material (binder) and embedded particles. The matrix material is used to provide structural support (and printability in additive manufacturing). The particles contain one or more materials to provide the desired properties such as electrical conductivity, thermal resistivity, magnetic permeability, etc. By adjusting the matrix material and particle properties and quantities, the properties of the composite can be optimized to attain the required functionality, rather than inventing a totally new material.

Because of their advantages, there have been many recent activities with particulate composites in extrusion based additive manufacturing, such as printing soft actuators with stretchable piezo electrical composites, circuit boards with conductive composites, multiple 3-D transforming structures with ferromagnetic material, and others [1-11]. Additional examples printed using Fiber Encapsulation Additive Manufacturing Technology in the LAMRA Lab at SMU include solenoids, voice coil actuators, switches, and a pressure/force sensor. [7-10].

During manufacturing, the particulate composites are melted into a particulate suspension inside the extruder. With the matrix material becoming a non-Newtonian suspension fluid, and

different types and number of particles distributed inside, the flow behavior is complex and may result in extruding difficulties and defects. For example, separation of the matrix material and particles may occur during extrusion on some processing conditions; the extruder may be blocked, and the device may be damaged when some combination of composites are used; and/or the manufactured products may not satisfy the property requirements. However, little theoretical or systematic research has been done on the behavior of the composite flow inside the extruder. Those difficulties are mostly overcome and solved inefficiently based on experience and by direct testing with different working conditions.

To solve the type of difficulty systematically, this paper will concentrate on the rheology of particulate composite flow in conditions approximating nozzle flow and discuss the factors that may impact the flow behavior. The primary interest is on the impact of particle volume fraction (Vol %), the nozzle/tube inside diameter (ID) D, and the particle mean size d.

2. Experiment

To quantify the rheology of the flow for the desired conditions (different particle volume fraction, different nozzle IDs and different particle mean size), a capillary rheometer has been designed and built as Fig. 1. A motorized linear stage (OpenBuild C-Beam® Linear Actuator Bundle and NEMA 23HS22-2804S-PG47 Stepper) with multiple syringes of 1 mL to 60 mL capacity is used to drive the flow. The capillaries are seamless steel tubing with IDs of 0.352, 0.409, 0.609, 0.843, 1.318, 1.7, and 2.01mm and different lengths. Omega Engineering PX61V1-1KGI and PX61v1-100GI pressure transducers are used for measuring the pressure required to drive the flow through the capillaries.

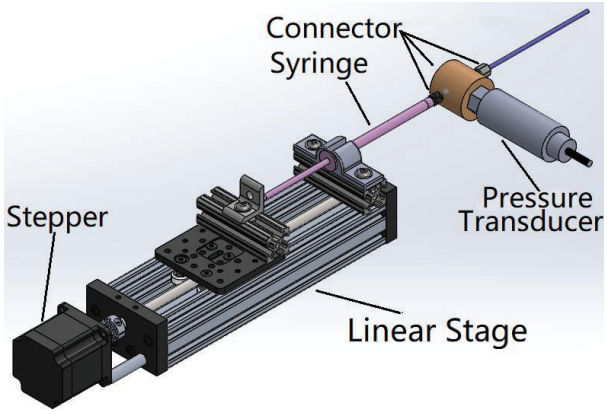

Fig. 1 Capillary rheometer

Within the rheometer, the flow rate Q can be controlled. When the flow arrives at steady state, the pressure drop in the capillary is collected from pressure transducer. To avoid the pressure measurement inaccuracy because of the contraction and developing region at the capillary entrance, tests are done on the capillaries with two different length (L1 and L2) for the same ID as Fig. 2. Then pressure drop ΔP in the fully developed length L can be attained by their difference. By testing with different flow rates, the wall shear stress τ_w, wall shear rate $\frac{du}{dr}_w$, and effective viscosity μ can be calculated from the following results [12]:

$$\tau_w = \frac{R}{2L}\Delta P = \frac{R}{2(L_1 - L_2)}(\Delta P_1 - \Delta P_2) \quad \ldots(1)$$

$$n = \frac{d(\ln(\frac{Q}{\pi R^3}))}{d(\ln(\tau_w))} \quad \ldots(2)$$

$$\frac{du}{dr}_w = \frac{4Q}{\pi R^3}\left(\frac{1}{4}n + \frac{3}{4}\right) \quad \ldots(3)$$

$$\mu = \frac{\tau_w}{\frac{du}{dr}_w} \quad \ldots(4)$$

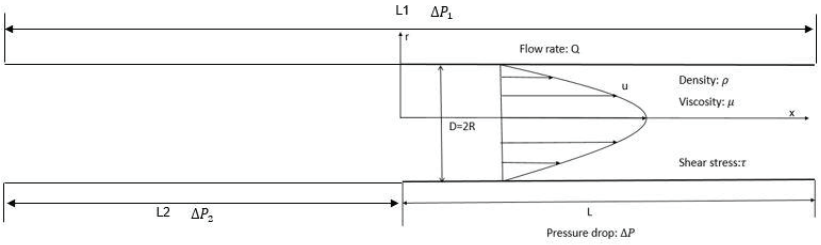

Fig. 2 Cross Section of Capillaries and the fully developed fluid profile

In the experiment, Momentive UV-Electro 225-1 Base silicone (a shear thinning material) is used as the matrix material instead of polymer melts to remove the impact of temperature and simplify the experiment. Two types of particles, Fibre Glast Microspheres 22 (d = 0.07 mm) and Spheriglass® Solid Glass Microspheres A3000 (d = 0.035 mm) were used to examine the impact of particles.

Based on collected data, it is found that n in equation (2) is constant for the same particulate suspension (made of the same type and volume fraction of material) in the capillary with the same ID. This is illustrated for a typical experiment in as Fig. 3. Thus, it can be concluded the type of flow follows a power law in which the shear stress can be described as

$$\tau = \boldsymbol{K}\dot{\gamma}^{\boldsymbol{n}} \quad \ldots(5)$$

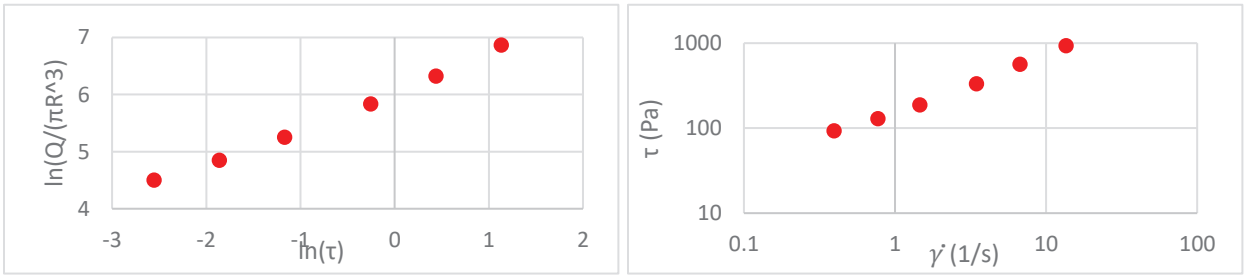

(a) (b)

Fig. 3 UV Electro 225-1 silicone and 20% A3000 particles (a) ln(Q/(πR^3)) vs. ln(τ), and (b) shear stress τ vs. shear rate $\dot{\gamma}$

Here, K is the flow consistency index and n is the flow behavior index. For a power-law fluid, the Reynolds number can be computed as [29]

$$Re = \frac{2^{7-3n}}{\pi^{2-n}}\left(\frac{n}{3n+1}\right)^n \frac{Q^{2-n}D^{3n-4}\rho}{K} \quad \ldots(6)$$

For this experiment, the Reynolds number is determined using equation (6) to be 0.006134, so the flow is laminar.

3. Data Analysis and Comparison with Similar Existing Models

Though particulate composites have been utilized in AM for many years without thorough investigation (as described above), related investigations for particle laden flows and suspensions in Newtonian fluids have been conducted for over 100 years as flow properties of suspensions are also an important topic in chemical reactions, the mining industry, and slurry transportation. Available literature [13-29] presents hundreds of equations trying to express relative viscosity of different types of suspensions of particles within a Newtonian fluid. Most of them are focused on the effects of particle volume fraction within free flow condition, with different kinds of considerations and limitations. Though there is a great variety of models and each has advantages and disadvantages, most of the models are similar. To simplify the discussion, the equations can be categorized into four fundamental types and combinations of them, including the original linear model, the polynomial model, the power law model, and the exponential model. Some of the important models are listed in Table 1 and discussed as examples below.

People/Time (type)	Equation
Einstein 1906	$\mu = \mu_0(1 + 2.5\phi_v)$
Guth, Eugene, & Simha 1936	$\mu = \mu_0(1 + 2.5\phi_v + 14.1\phi_v^2)$
Mooney 1951 (semi-empirical)	$\mu = \mu_0 \exp(\frac{2.5\phi_v}{1 + k\phi_v})$
Simha 1952 (semi-empirical)	$\mu = \mu_0(1 + 1.5\phi_v(1 + (1 + (25\phi_v/4f^3) \ldots))$
Krieger & Dougherty 1959 (semi-empirical)	$\mu = \mu_0 \frac{1}{(1 - \frac{\phi_v}{\phi_M})^{[\mu]\phi_M}}$
Ford 1960 (semi-empirical)	$\mu = \mu_0(1 + 2.5\phi_v + 11\phi_v^5 - 11.5\phi_v^7)$
Quemada 1978 (semi-empirical)	$\mu = \mu_0(1 - \frac{\phi_v}{\phi_m})$
Snapati 2009 (semi-empirical)	$\mu = \mu_0 \frac{10C_U}{d_{50}}[1 + \frac{[\mu]}{\dot{\gamma}^{0.4}}\left(\frac{\phi_v}{\phi_m - \phi_v}\right)]^{3.5}$
Blissett 2013 (semi-empirical)	$\mu = \mu_0 \left(1 - \frac{\phi_v}{\phi_M}\right)^{-[\mu]\phi_M} + m(\phi_v)\dot{\gamma}^{n(\dot{\phi}_v)-1}$

Table 1 Significant Relative Viscosity Models. Here μ is the suspension viscosity, μ_0 is the matrix material viscosity, $\phi_v$is particle volume fraction, ϕ_M is the maximum particle volume fraction (i.e., the maximum achievable particle volume fraction), [μ] is the intrinsic viscosity, the others are empirical constants

Comparison of several relative viscosity models with the measured data for non-Newtonian matrix material is shown in Fig. 4. In general, the models do not agree with the measured data. The flow consistency index has the similar trend as the measured results, however, the accuracy

decreases dramatically as the particle volume fraction increases. Also, the flow behavior index change is not captured by these models. It is believed that the reason is the existing models are focused on Newtonian suspension fluid at free flow conditions.

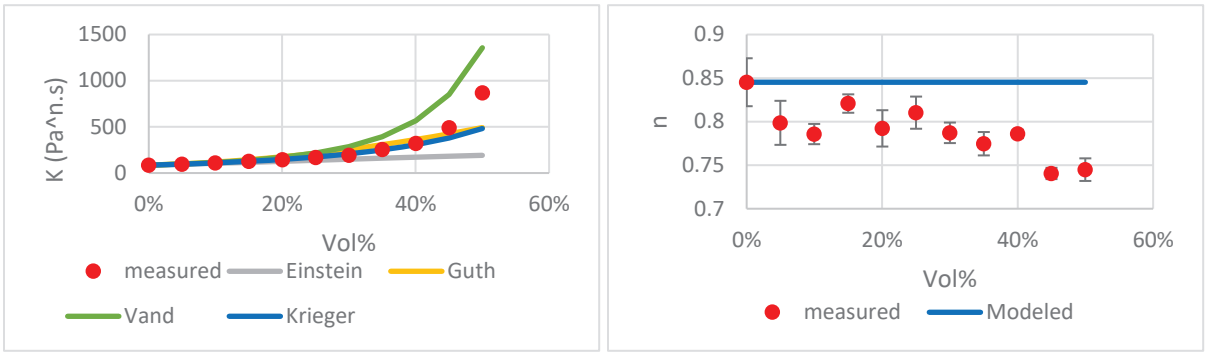

(a) (b)

Fig. 4 Flow behavior for the free flow condition (large D) vs. Particle volume fraction Vol% (a) Flow consistency index K, and (b) Flow behavior index n. The material is Momentive UV-Electro 225-1 Base silicone + 30% particles with d= 0.035 mm. Each point is the average of 5 test measurement results. Each testing result is calculated from 6 different shear rates in the range 0.5 to 15 1/s, as shown in Fig. 4.

Another factor that impacts the flow behavior is the capillary inside diameter and particle mean size ratio (D/d) as shown in Fig. 5 (taking flow with 30% particles as an example). It is visible that the flow consistency index is almost constant when the ratio is larger than 50, decreases as D/d decreases between 20 and 50, and then increases as D/d continuies to decrease below 20 until the nozzle blocked when D/d is around 3 or smaller. The flow behavior index does not change significantly and is regarded as constant for the conditions investigated.

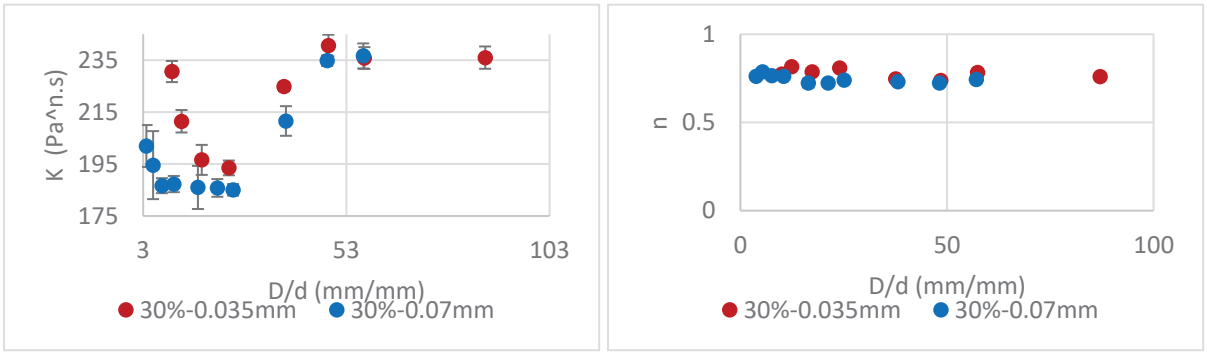

(a) (b)

Fig. 5 Flow behavior vs. Capillary ID/Particle mean size (D/d) (a) Flow consistency index K, and (b) Flow behavior index n. The material flow is Momentive UV-Electro 225-1 Base silicone + 30% particles with d= 0.035/0.07 mm. Each point is the average of 5 testing measurement results. Each testing result is calculated from 6 different shear rates in the range 0.5 to 15 1/s as shown in Fig. 4.

The behavior of K can be illustrated with the schematics shown in Fig. 6.

- When the D/d ratio is larger than 50, there is enough space between particles or particles and the wall, that the particles have minimal interaction with their surroundings and the flow is at free flow condition. Thus, the flow consistency index is constant with little impact from the capillary tube.
- When the D/d ratio is between 20 and 50, interaction occurs among particles and wall. Since the wall is fixed, a key effect of the wall is to push particles away from it so that collisions with the wall tend to push particles into the center of the capillary. As a result, there is a higher concentration of suspension fluid near the wall, which tends to lower shear stress and the flow consistency index, K. At this ratio range, the results suggest a smaller D/d ratio tends to strengthen the particle centering effect, resulting in a reduced K. This condition is called the particle & wall interaction condition.
- When D/d is between 3 and 20, there is not enough space for the particles to go smoothly through the capillaries. With the smaller ratio, there are smaller space, and it is easier for the particles to interfere with each other, which results in a larger flow consistency index. This is called the particle interaction condition.
- One interesting phenomenon happening at the particle interaction condition is the flow consistency index may vary a lot when the D/d ratio is the same but types of particles are different. This may be due to different particle size distributions. For example, the particles with a mean size of 0.035 mm may have a wider size distribution than the particles with a mean size of 0.07 mm. Relatively larger particles from a wider size distribution may induce jamming more easily. This may explain why the flow consistency index of particles with the mean size of 0.035 mm is much larger than the mean size of 0.07 mm, as indicated Fig. 6 (a), for D/d < 20.
- When the D/d ratio is around 3 or smaller, particles are much easier to gather together and span the entire capillary. Then it is impossible to move the flow with the original pressure. The capillary is blocked, in which case the jamming condition is achieved.

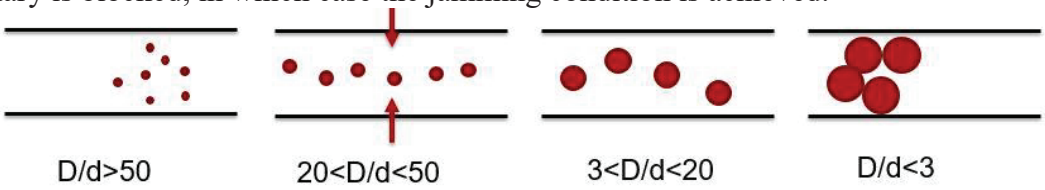

Fig. 6 Particle capillary size ratio impacts (based on Momentive UV-Electro 225-1 Base silicone + 30% particles with d= 0.035/0.07 mm) (a) free flow condition (b) particle & wall interaction condition (c) jamming starting condition (d) jamming condition

4. Conclusion & Application in Additive Manufacturing

This experimental study shows how the particle volume fraction, capillary ID and particle mean size impacts the flow behavior when the suspension fluid is non-Newtonian and the particle diameter is on the micrometer scale. The reasons for the phenomena are also discussed. One possible relationship between flow consistency index and particle size distribution is also proposed.

These results may help avoid undesirable flow conditions and nozzle blockage during particulate composite printing. The printing quality may also be improved.

Acknowledgements

This paper is based on work supported by the National Science Foundation under grant no. 1317961. Research was performed at the Laboratory for Additive Manufacturing, Robotics, and Automation, Department of Mechanical Engineering, Southern Methodist University, Dallas, Texas. The authors appreciate the assistance of Drs. Matt Saari and Daniel Porter.

Author Disclosure Statement

The authors have no financial conflicts.

Reference

[1] Miriyev, Aslan, Kenneth Stack, and Hod Lipson. "Soft material for soft actuators." *Nature Communications* 8 (2017).

[2] Wehner, Michael, et al. "An integrated design and fabrication strategy for entirely soft, autonomous robots." *Nature* 536.7617 (2016): 451-455.

[3] Sun, Ke, et al. "3D printing of interdigitated Li‐Ion microbattery architectures." *Advanced Materials* 25.33 (2013): 4539-4543.

[4] Coronel, Jose L., et al. "Increasing component functionality via multi-process additive manufacturing." *Micro-and Nanotechnology Sensors, Systems, and Applications IX*. Vol. 10194. International Society for Optics and Photonics, 2017.

[5] Tibbits, Skylar. "4D printing: multi‐material shape change." *Architectural Design* 84.1 (2014): 116-121.

[6] Leigh, Simon J., et al. "A simple, low-cost conductive composite material for 3D printing of electronic sensors." *PloS one* 7.11 (2012): e49365.

[7] Saari, Matt, et al. "Fabrication and Analysis of a Composite 3D Printed Capacitive Force Sensor." *3D Printing and Additive Manufacturing* 3.3 (2016): 136-141.

[8] Cox, Bryan, et al. "Fiber Encapsulation Additive Manufacturing: Technology and Applications Update." *3D Printing and Additive Manufacturing* 4.2 (2017): 116-119.

[9] Saari, Matt, et al. "Additive Manufacturing of Soft Parts from Thermoplastic Elastomers."

[10] Xia B, Saari M, Cox B, Richer E, Krueger PS, Cohen AL, (2016). " Fiber Encapsulation Additive Manufacturing: Materials for Electrical Junction Fabrication," Solid Freeform Fabrication Symposium. 2016. Austin, TX, Austin, TX: University of Texas at Austin; 2015, 1345-1358.

[11] Clay, Collin. *Electrically conductive thermoplastic elastomers in application to additive manufacturing*. Diss. Southern Methodist University, 2014.

[12] Chhabra, Raj P., and John Francis Richardson. *Non-Newtonian flow and applied rheology: engineering applications*. Butterworth-Heinemann, 2011.

[13] Einstein, Albert "Investigations on the Theory of the Brownian Movement: DoverPublications. com." *New York* 58 (1956).

[14] Jeffrey, Duncan James, and Andreas Acrivos. "The rheological properties of suspensions of rigid particles." *AIChE Journal*22.3 (1976): 417-432.

[15] Guth, Eugene, and R. Simha. "Untersuchungen über die viskosität von suspensionen und lösungen. 3. über die viskosität von kugelsuspensionen." *Colloid & Polymer Science*74.3 (1936): 266-275.

[16] Vand, Vladimir. "Viscosity of solutions and suspensions. I. Theory." *The Journal of Physical Chemistry* 52.2 (1948): 277-299.

[17] Mooney, Melvin. "The viscosity of a concentrated suspension of spherical particles." *Journal of colloid science* 6.2 (1951): 162-170.

[18] Simha, Robert. "A treatment of the viscosity of concentrated suspensions." *Journal of Applied physics* 23.9 (1952): 1020-1024.

[19] Brinkman, H. C. "The viscosity of concentrated suspensions and solutions." *The Journal of Chemical Physics* 20.4 (1952): 571-571.

[20] Krieger, Irvin M., and Thomas J. Dougherty. "A mechanism for non‐Newtonian flow in suspensions of rigid spheres." *Transactions of the Society of Rheology* 3.1 (1959): 137-152.

[21] Ford, T. F. "Viscosity-concentration and fluidity-concentration relationships for suspensions of spherical particles in Newtonian liquids." *The Journal of Physical Chemistry* 64.9 (1960): 1168-1174.

[22] Thomas, David G. "Transport characteristics of suspension: VIII. A note on the viscosity of Newtonian suspensions of uniform spherical particles." *Journal of Colloid Science* 20.3 (1965): 267-277.

[23] Batchelor, G. K. "The effect of Brownian motion on the bulk stress in a suspension of spherical particles." *Journal of fluid mechanics* 83.1 (1977): 97-117.

[24] Quemada, D. "Rheology of concentrated disperse systems II. A model for non-Newtonian shear viscosity in steady flows." *Rheologica Acta* 17.6 (1978): 632-642.

[25] Wildemuth, C. R., and M. C. Williams. "Viscosity of suspensions modeled with a shear-dependent maximum packing fraction." *Rheologica acta* 23.6 (1984): 627-635.

[26] Bournonville, B., and A. Nzihou. "Rheology of non-Newtonian suspensions of fly ash: effect of concentration, yield stress and hydrodynamic interactions." *Powder technology* 128.2-3 (2002): 148-158.

[27] Senapati, P. K., B. K. Mishra, and A. Parida. "Modeling of viscosity for power plant ash slurry at higher concentrations: Effect of solids volume fraction, particle size and hydrodynamic interactions." *Powder Technology* 197.1-2 (2010): 1-8.

[28] Blissett, R. S., and N. A. Rowson. "An empirical model for the prediction of the viscosity of slurries of coal fly ash with varying concentration and shear rate at room temperature." *Fuel* 111 (2013): 555-563.

[29] Christopher, Robert H., and Stanley Middleman. "Power-law flow through a packed tube." *Industrial & Engineering Chemistry Fundamentals* 4.4 (1965): 422-426.